Identifying Peru's Business Cycles: A Bayesian Approach

F. Martin Martinez P.

November 2022

Abstract

This paper applies the unobserved–components framework of Chan and Grant (2018b) to decompose Peru's real GDP (1980Q1–2018Q4) into trend and cycle. Using a specification with a random-walk trend in growth and an AR(2) output gap with potentially correlated innovations, the estimates outperform alternative methods in statistical fit and historical coherence. The results indicate negative potential growth in the late 1980s, a strong recovery during the 1990s, and a post-2008 deceleration. Based on the estimated gap, we date five cycles,four complete and one ongoing as of 2018Q4 (the end of the sample), with durations between 21 and 45 quarters, and we document a marked decline in cyclical volatility since the late 1990s, consistent with a more stable macroeconomic environment.

Keywords: Unobserved components, Business cycles, Bayesian estimation, Potential GDP.

1. Introduction

The decomposition of Gross Domestic Product (GDP) into cyclical and trend components is a statistical and conceptual problem of first-order importance: it is essential both for studying recessions and recurrent expansions in market economies and for designing and implementing monetary policy. *Potential output*[1] can be defined as the level of production in an economy without distortions and without generating inflationary pressures, while the *output gap* is the percentage deviation of GDP from its potential.

From a statistical perspective, most macroeconomic variables such as GDP have at least one unit root, i.e., they feature stochastic trends. Conceptually, the trend component of GDP is associated with long-run, flexible-price frequencies where there are no inflationary pressures from aggregate demand. By contrast, the cyclical component is tied to short-run dynamics with nominal rigidities, where monetary policy has real effects. In this context, the business cycle is defined as the percentage deviation of GDP from its trend component.

Decomposing GDP helps assess the economy's position relative to its long-run trend and to identify the duration and extent of expansions and recessions. A wide variety of methodologies exists to estimate this decomposition, and they can yield disparate estimates that need not reflect a country's historical evolution of economic activity.

The literature offers many proposals for trend-cycle decomposition of GDP[2]. Among the main univariate approaches are the Hodrick–Prescott (HP) filter (Hodrick and Prescott, 1997), Beveridge and Nelson (1981), Baxter and King (1999), and unobserved components (UC) models (Harvey, 1985; Watson, 1986; Clark, 1987), among others. The diversity of estimates has generated debate about the sources of differences and their incompatibilities with countries chronological characteristics. For the United States, Morley et al. (2003) reconciled the results of Beveridge and Nelson (1981) and the UC model of Clark (1987) by allowing correlation between innovations to potential output and the output gap. Later, Chan and Grant (2018a) show that the differences between Morley's estimates and those of the HP filter are due to alternative specifications of the potential output and output gap.

For Peru, applications span both univariate and multivariate frameworks (Cabredo and Valdivia, 1998; Llosa and Miller, 2005; Rodríguez, 2009). Miller (2003) reviews the main methods and finds that, regardless of the approach, potential output growth would have turned negative in the late 1980s, when the country faced its deepest economic and social crisis. However, Guillén and Rodríguez (2014) followed an alternative approach based on mixtures of normals, proposed by Perron and Wada (2009), finding that potential growth at the end of that decade remained positive—though lower than later decades—and more stable. Although there is no clear consensus, the crisis is widely understood to have reduced capital,

[1] An alternative definition is the level of production reached in an economy where all markets are competitive.

[2] Chagny y Doepke (2001) estimate trend–cycle decompositions, under a variety of methods, for Eurozone countries.

employment, and total factor productivity, implying negative potential growth during that period.

Building on these considerations, this paper applies the approach of Chan and Grant (2018b) to estimate potential output growth, yielding results that are consistent with Peru's late-1980s crisis and an output gap that coheres with documented historical episodes. The methodology is an unrestricted UC model that allows correlation between innovations to the output gap (transitory component) and the trend (permanent component) within a Bayesian framework, leveraging band- and sparse-matrix algorithms for state-space models developed by Chan and Jeliazkov (2009)[3]. These algorithms are more efficient than Kalman filter–based methods and render exact computation of the integrated (marginal) likelihood feasible for Bayesian model comparison (McCausland et al., 2010; Chan and Eisenstat, 2015).

This paper is organized as follows. Section 2 reviews UC specifications and the framework of Chan and Grant (2018b); Section 3 reports estimation results and compares models; Section 4 examines the preferred model's trend and gap estimates and dates Peru's business cycles; and Section 5 concludes.

2. Empirical strategy

In the first part of this section, I present the methodology developed by Chan and Grant (2018b), alongside alternative specifications from the unobserved-components literature within a Bayesian framework. These models rest on the idea that an observed series can be decomposed into two parts: a stationary transitory component, the output gap, and a nonstationary permanent component, the trend or potential output.

$$y_t = \tau_t + c_t, \qquad t = 1, \ldots, T. \tag{1}$$

where seasonally adjusted real log GDP y_t (Peru, quarterly, 1980–2018) is the sum of a nonstationary permanent component (potential output, τ_t) and a stationary transitory component (the output gap, c_t). Each component is modeled independently.

Following Clark (1987); Watson (1986), the output gap is a mean-zero stationary AR(2):

$$c_t = \phi_1 c_{t-1} + \phi_2 c_{t-2} + u_t^c, \qquad u_t^c \sim \mathcal{N}(0, \sigma_c^2). \tag{2}$$

where c_t denotes the transitory component, ϕ_1 and ϕ_2 are persistence parameters, and u_t^c is the innovation (shock) to the transitory component.

By contrast, the specification of the permanent component is a key source of methodological

[3]In a multivariate setting, the integrated likelihood can be computed exactly, overcoming computational issues that arise with approximations; the algorithm also facilitates comparisons between univariate and multivariate models.

variation within UC models. The formulation proposed by Chan and Grant (2018b)[4] follows a second–order Markov process in Equation (3).

$$\Delta\tau_t = \Delta\tau_{t-1} + u_t^\tau, \qquad u_t^\tau \sim \mathcal{N}(0, \sigma_\tau^2). \tag{3}$$

where $\Delta\tau_t$ denotes the growth rate of the permanent component (potential output) and u_t^τ is its innovation. This specification treats innovations to potential growth as long-run shocks that shape the series' trend. A second source of methodological variation concerns whether innovations to the transitory and permanent components are correlated. We allow for this by assuming the shocks $(u_t^c, u_t^\tau)'$ are jointly normal with correlation ρ:

$$\begin{pmatrix} u_t^c \\ u_t^\tau \end{pmatrix} \sim \mathcal{N}\left(\begin{pmatrix} 0 \\ 0 \end{pmatrix}, \begin{pmatrix} \sigma_c^2 & \rho\,\sigma_c\sigma_\tau \\ \rho\,\sigma_c\sigma_\tau & \sigma_\tau^2 \end{pmatrix} \right), \qquad \rho \in (-1, 1). \tag{4}$$

where ρ denotes the correlation between innovations to the output gap and to potential output.

The methodology has evolved since the pioneering contributions of Harvey (1985), Watson (1986), and Clark (1987), and the resulting approaches differ along the two dimensions noted above: (i) the specification of the permanent component and (ii) the treatment of correlation between innovations to the transitory and permanent components. Common specifications for the trend include a random walk with time-varying drift (Clark, 1987), a random walk with constant drift (e.g., Morley et al. (2003)), and a random walk with drift allowing up to two exogenous breaks (Chan and Grant, 2018a). These models are typically labeled UC (unobserved components) or UCUR (unrestricted unobserved components). The next table summarizes these specifications and their assumptions regarding the correlation between innovations to the output gap and the trend.

[4] Chan and Grant (2018b) adopt an alternative specification for potential output to reconcile differences between UC estimates and those from the Hodrick–Prescott filter. In their setup, the HP filter emerges as a special case when: (i) the innovations to the gap and the trend are uncorrelated; (ii) the gap follows a random walk; and (iii) the smoothness parameter equals the volatility ratio of the gap to the trend.

Table 1: Model specifications

Model	**Permanent component**	
UC0 – Clark (1987)	$\tau_t = \mu_t + \tau_{t-1} + \varepsilon_t^\tau$ $\mu_t = \mu_{t-1} + \varepsilon_t^\mu$	$\begin{pmatrix}\varepsilon_t^c \\ \varepsilon_t^\tau\end{pmatrix} \sim \mathcal{N}\left(\begin{pmatrix}0\\0\end{pmatrix}, \begin{pmatrix}\sigma_c^2 & 0 \\ 0 & \sigma_\tau^2\end{pmatrix}\right)$
UCUR – Morley (2003) **UCUR-1 – Chan (2018a)** **UCUR-2 – Chan (2018a)**	$\tau_t = \mu + \tau_{t-1} + \varepsilon_t^\tau$ $\tau_t = \mu_1 + \tau_{t-1} + \varepsilon_t^\tau$ $\tau_t = \mu_1 + \mu_2 + \tau_{t-1} + \varepsilon_t^\tau$	$\begin{pmatrix}\varepsilon_t^c \\ \varepsilon_t^\tau\end{pmatrix} \sim \mathcal{N}\left(\begin{pmatrix}0\\0\end{pmatrix}, \begin{pmatrix}\sigma_c^2 & \rho\sigma_c\tilde{\sigma}_\tau \\ \rho\sigma_c\tilde{\sigma}_\tau & \sigma_\tau^2\end{pmatrix}\right)$
Perron and Wada (2013)	$\tau_t = \tau_{t-1} + \mu_t + \varepsilon_t^\tau$ $\mu_t = \mu_{t-1} + \varepsilon_t^\mu$	$\varepsilon_t^\mu = \lambda_t\gamma_{1t} + (1-\lambda_t)\gamma_{2t}$
UCUR2M – Chan (2018b)	$\Delta\tau_t = \Delta\tau_{t-1} + u_t^\tau$	$\begin{pmatrix}\varepsilon_t^c \\ \varepsilon_t^\tau\end{pmatrix} \sim \mathcal{N}\left(\begin{pmatrix}0\\0\end{pmatrix}, \begin{pmatrix}\sigma_c^2 & \rho\sigma_c\tilde{\sigma}_\tau \\ \rho\sigma_c\tilde{\sigma}_\tau & \sigma_\tau^2\end{pmatrix}\right)$
Special cases:		
UC2M	$\Delta\tau_t = \Delta\tau_{t-1} + u_t^\tau$, $\hat{\lambda} = \dfrac{\sigma_c^2}{\sigma_\tau^2}$	$\begin{pmatrix}\varepsilon_t^c \\ \varepsilon_t^\tau\end{pmatrix} \sim \mathcal{N}\left(\begin{pmatrix}0\\0\end{pmatrix}, \begin{pmatrix}\sigma_c^2 & 0 \\ 0 & \sigma_\tau^2\end{pmatrix}\right)$
HP + AR(2)	$\Delta\tau_t = \Delta\tau_{t-1} + u_t^\tau$, $\lambda = 1600$	
HP-UC	$\Delta\tau_t = \Delta\tau_{t-1} + u_t^\tau, \quad \lambda = 1600$	

In Table 1, UCUR-1 and UCUR-2 allow for one and two break points, respectively. For Peru, estimates from UC0, UCUR, UCUR-1, and UCUR-2 are generally unpromising because they fail to capture key historical episodes. This shortcoming likely reflects the presence of (at least) two structural breaks in the Peruvian economy (Guillén and Rodríguez, 2014), which even the two-break UCUR-2 specification does not accommodate satisfactorily in practice.

HP–UC is the unobserved–components representation of the Hodrick–Prescott filter with the smoothness parameter fixed at $\lambda = 1600$ (see Chan and Grant (2018b), Appendix B). In this specification, the transitory component has no persistence and the innovations to the transitory and permanent components are assumed to be uncorrelated. The HP–AR variant augments HP–UC by estimating the persistence (e.g., AR(2)) of the transitory component. By contrast, UC2M models the permanent component as a random walk in the growth rate (i.e., trend growth follows a random walk). Finally, UCUR2M (Chan and Grant, 2018b) extends UC2M by allowing a nonzero covariance between innovations—equivalently, correlation—across the transitory (gap) and permanent (trend) components.

Additionally, Table 1 reports the application by Guillén and Rodríguez (2014) of the methodology developed by Perron and Wada (2009). This approach extends the UCUR model with a two–component normal mixture estimated by maximum likelihood. This methodology provides an interesting contribution to the existing literature by adding the

idea that each innovation is drawn from one of two normal distributions.

In this subsection, we outline the estimation of UCUR2M based on Equations (1) to (3), following the procedure in Chan and Grant (2018b). The approach (i) incorporates prior information via weakly informative priors on the parameters $\phi_1, \phi_2, \sigma_c^2, \sigma_\tau^2, \rho, \tau_0, \tau_{-1}$, and (ii) exploits the banded and sparse linear–algebra routines of Chan and Jeliazkov (2009), which deliver speed gains of roughly 20–40% over Kalman filter–based methods (McCausland et al., 2010).

We employ a six–block Gibbs sampler to draw from the joint posterior $p(\tau, \phi, \sigma_c^2, \sigma_\tau^2, \rho, \tau_0, \tau_{-1} \mid y)$. Initialize at $\phi^{(0)} \in \mathbb{R}$, $\sigma_c^{2(0)} > 0$, $\sigma_\tau^{2(0)} > 0$, $-1 < \rho^{(0)} < 1$, $(\tau_0^{(0)}, \tau_{-1}^{(0)}) = (y_1, y_1)$, where $\mathbb{R}$ is the stationarity region for (ϕ_1, ϕ_2) and y_1 denotes the first observation. Then, for $r = 1, \ldots, R$, iterate the following blocks:

1) $p(\tau \mid y, \phi, \sigma_c^2, \sigma_\tau^2, \rho, \tau_0, \tau_{-1})$ *multivariate normal*

2) $p(\phi \mid y, \tau, \sigma_c^2, \sigma_\tau^2, \rho, \tau_0, \tau_{-1})$ *normal*

3) $p(\sigma_c^2 \mid y, \tau, \phi, \sigma_\tau^2, \rho, \tau_0, \tau_{-1})$ *uniform*

4) $p(\sigma_\tau^2 \mid y, \tau, \phi, \sigma_c^2, \rho, \tau_0, \tau_{-1})$ *uniform*

5) $p(\rho \mid y, \tau, \phi, \sigma_c^2, \sigma_\tau^2, \tau_0, \tau_{-1})$ *uniform*

6) $p(\tau_0, \tau_{-1} \mid y, \tau, \phi, \sigma_c^2, \sigma_\tau^2, \rho)$ *normal*

Before computing our hybrid Gibbs sampler, we rewrite Equations (1) to (3) in state–space form:

$$y_{T\times 1} \;=\; \tau_{T\times 1} \;+\; c_{T\times 1} \tag{5}$$

$$(\mathbf{H}_\phi)_{T\times T}\, c_{T\times 1} \;=\; u^c_{T\times 1} \tag{6}$$

$$(\mathbf{H_2})_{T\times T}\, \tau_{T\times 1} \;=\; \tilde{\alpha}_{T\times 1} \;+\; u^\tau_{T\times 1} \tag{7}$$

where $\tilde{\alpha} = (\, 2\tau_0 - \tau_{-1},\, -\tau_0,\, 0,\, \ldots,\, 0\,)'$ and

$$\mathbf{H}_2 = \begin{pmatrix} 1 & 0 & 0 & \cdots & 0 \\ -2 & 1 & 0 & \cdots & 0 \\ 1 & -2 & 1 & \cdots & 0 \\ \vdots & \ddots & \ddots & \ddots & \vdots \\ 0 & \cdots & 1 & -2 & 1 \end{pmatrix}, \qquad \mathbf{H}_\phi = \begin{pmatrix} 1 & 0 & 0 & \cdots & 0 \\ -\phi_1 & 1 & 0 & \cdots & 0 \\ -\phi_2 & -\phi_1 & 1 & \cdots & 0 \\ \vdots & \ddots & \ddots & \ddots & \vdots \\ 0 & \cdots & -\phi_2 & -\phi_1 & 1 \end{pmatrix}.$$

Both $\mathbf{H}_2$ and $\mathbf{H}_\phi$ are lower–triangular band matrices with nonzero entries concentrated near the diagonal. Since their diagonals are unity, $\det(\mathbf{H}_2) = \det(\mathbf{H}_\phi) = 1$, and thus both matrices are invertible.

Likewise, we assume the following prior distributions for the parameters to be estimated:

$$\phi \sim \mathcal{N}(\phi_0, V_\phi)\,\mathbf{1}\{\phi \in \mathbb{R} \qquad (\tau_0, \tau_{-1}) \sim \mathcal{N}(\tau_0, V_t)$$

where $\mathbb{R}$ denotes the stationary region for (ϕ_1, ϕ_2), $\phi = (\phi_1, \phi_2)'$ collects the persistence parameters of the output gap and is assigned a truncated normal prior on the stationarity region $\mathbb{R}$, i.e., $\phi \sim \mathcal{N}(\phi_0, V_\phi)\,\mathbf{1}\{\phi \in \mathbb{R}$, with a diffuse variance $V_\phi = \mathbb{I}_2$ to cover a wide range of values. Because the initial level of the permanent component is unknown, the first two states are estimated under a normal prior, $(\tau_0, \tau_{-1})' \sim \mathcal{N}\big((\tau_{00}, \tau_{00})',\, V_\tau\, \mathbb{I}_2\big)$, with prior mean τ_{00} and variance V_τ.

The innovation variances are assigned independent uniform priors on the positive support:

$$\sigma_c^2 \sim \mathcal{U}(0, b_c) \qquad \sigma_\tau^2 \sim \mathcal{U}(0, b_\tau)$$

with hyperparameters $b_c, b_\tau > 0$ reflecting prior bounds on volatility.

The correlation coefficient[5] between the innovations naturally lies in $(-1, 1)$; accordingly, we set

$$\rho \sim \mathcal{U}(-1, 1)$$

Hence, conditional on ϕ, σ_c^2, σ_τ^2, and (τ_0, τ_{-1}), we have:

$$\begin{pmatrix} c \\ \tau \end{pmatrix} \sim \mathcal{N}\left(\begin{pmatrix} 0 \\ \alpha \end{pmatrix}, \begin{pmatrix} \sigma_c^2\,(\mathbf{H}_\phi'\mathbf{H}_\phi)^{-1} & \rho\,\sigma_c\sigma_\tau\,(\mathbf{H}_\phi'\mathbf{H}_2)^{-1} \\ \rho\,\sigma_c\sigma_\tau\,(\mathbf{H}_\phi'\mathbf{H}_2)^{-1} & \sigma_\tau^2\,(\mathbf{H}_2'\mathbf{H}_2)^{-1} \end{pmatrix} \right),$$

where $\alpha = \mathbf{H}_2^{-1}\tilde{\alpha}$. By standard properties of the multivariate normal, the marginal distribution of τ (unconditional on c) is:

$$(\tau \mid \sigma_\tau^2, \tau_0, \tau_{-1}) \sim \mathcal{N}\big(\alpha,\ \sigma_\tau^2\,(\mathbf{H}_2'\mathbf{H}_2)^{-1}\big)\,,$$

and the conditional distribution of y given τ and the other parameters is:

$$\big(y \mid \tau, \phi, \sigma_c^2, \sigma_\tau^2, \rho, \tau_0, \tau_{-1}\big) \sim \mathcal{N}\big(\mathbf{H}_\phi^{-1}\mathbf{a} + \mathbf{H}_\phi^{-1}\mathbf{B}\,\tau,\ (1-\rho^2)\,\sigma_c^2\,(\mathbf{H}_\phi'\mathbf{H}_\phi)^{-1}\big)\,,$$

where $\mathbf{a} = \dfrac{\rho\,\sigma_c}{\sigma_\tau}\,\mathbf{H}_2\alpha$ and $\mathbf{B} = \mathbf{H}_\phi + \dfrac{\rho\,\sigma_c}{\sigma_\tau}\,\mathbf{H}_2$.

Thus, the prior density of τ and the conditional likelihood are given by:

$$p(\tau \mid \sigma_\tau^2, \tau_0, \tau_{-1}) = (2\pi\sigma_\tau^2)^{-T/2} \exp\left\{ -\frac{1}{2\sigma_\tau^2}\,(\tau - \alpha)'\mathbf{H}_2'\mathbf{H}_2(\tau - \alpha) \right\},$$

[5] If potential output were modeled as a time-varying random walk, $\tau_t = \beta_t + \tau_{t-1} + \mu_t^\tau$, with zero correlation, all UC estimates would coincide with Clark's methodology.

$$p(y \mid \tau, \phi, \sigma_c^2, \sigma_\tau^2, \rho, \tau_0, \tau_{-1}) = \left(2\pi\,\sigma_c^2(1-\rho^2)\right)^{-T/2} \exp\left\{-\frac{(\mathbf{H}_\phi y - \mathbf{a} - \mathbf{B}\tau)'(\mathbf{H}_\phi y - \mathbf{a} - \mathbf{B}\tau)}{2(1-\rho^2)\,\sigma_c^2}\right\}.$$

Using standard linear regression results, we get:

$$(\tau \mid y, \phi, \sigma_c^2, \sigma_\tau^2, \rho, \tau_0, \tau_{-1}) \sim \mathcal{N}\big(\hat{\tau},\ \mathbf{K}_\tau^{-1}\big),$$

where

$$\mathbf{K}_\tau \;=\; \frac{1}{\sigma_\tau^2}\,\mathbf{H}_2'\mathbf{H}_2 \;+\; \frac{1}{(1-\rho^2)\,\sigma_c^2}\,\mathbf{B}'\mathbf{B},$$

and

$$\hat{\tau} \;=\; \mathbf{K}_\tau^{-1}\left(\frac{1}{\sigma_\tau^2}\mathbf{H}_2'\mathbf{H}_2\alpha \;+\; \frac{1}{(1-\rho^2)\,\sigma_c^2}\,\mathbf{B}'\left(\mathbf{H}_\phi y - \mathbf{a}\right)\right).$$

Since $\mathbf{H}_2$ and $\mathbf{H}_\phi$ are banded, the resulting $\mathbf{K}_\tau$ is a sparse precision matrix, which enables efficient sampling via the precision sampler of Chan and Jeliazkov (2009).

To sample ϕ in step 2, we note that u^c and τ are jointly normal:

$$\begin{pmatrix} u^c \\ \tau \end{pmatrix} \sim \mathcal{N}\left(\begin{pmatrix} 0 \\ \alpha \end{pmatrix}, \begin{pmatrix} \sigma_c^2\,\mathbf{I}_T & \rho\,\sigma_c\sigma_\tau\,(\mathbf{H}_2')^{-1} \\ \rho\,\sigma_c\sigma_\tau\,(\mathbf{H}_2)^{-1} & \sigma_\tau^2\,(\mathbf{H}_2'\mathbf{H}_2)^{-1} \end{pmatrix}\right),$$

recall that $\alpha = \mathbf{H}_2^{-1}\,\tilde{\alpha}$. Hence, the conditional distribution of u^c given τ y the other parameters is

$$\left(u^c \mid \tau, \sigma_c^2, \sigma_\tau^2, \rho, \tau_0, \tau_{-1}\right) \sim \mathcal{N}\left(\frac{\rho\,\sigma_c}{\sigma_\tau}\,\mathbf{H}_2(\tau - \alpha),\ (1-\rho^2)\,\sigma_c^2\,\mathbf{I}_T\right)$$

Then, we rewrite Equation (2) as:

$$c \;=\; \mathbf{X}_\phi\,\phi \;+\; u^c$$

where $\mathbf{X}_\phi$ is a $T \times 1$ matrix consisting of lagged values of c_t. By standard regression results we obtain

$$\left(\phi \mid y, \tau, \sigma_c^2, \sigma_\tau^2, \rho, \tau_0, \tau_{-1}\right) \sim \mathcal{N}\big(\hat{\phi},\ \mathbf{K}_\phi^{-1}\big)\ \mathbf{1}\{\phi \in \mathbb{R}$$

where

$$\mathbf{K}_\phi \;=\; \mathbf{V}_\phi^{-1} \;+\; \frac{1}{(1-\rho^2)\,\sigma_c^2}\,\mathbf{X}_\phi'\,\mathbf{X}_\phi$$

and

$$\hat{\phi} \;=\; \mathbf{K}_\phi^{-1}\left(\mathbf{V}_\phi^{-1}\phi_0 \;+\; \frac{1}{(1-\rho^2)\,\sigma_c^2}\,\mathbf{X}_\phi'\left[c \;-\; \frac{\rho\,\sigma_c}{\sigma_\tau}\,\mathbf{H}_2\,(\tau - \alpha)\right]\right).$$

A draw from this truncated normal distribution can be obtained by an acceptance–rejection scheme (keep sampling until $\phi \in \mathbb{R}$).

To implement steps 3 and 4, we first derive the joint density of u^c and u^τ. Using σ_c^2 and

σ_τ^2, we have the joint distribution of (u^c, u^τ):

$$u_t^\tau \sim \mathcal{N}(0, \sigma_\tau^2) \qquad ; \qquad \left(u_t^c \mid u_t^\tau\right) \sim \mathcal{N}\left(\frac{\rho\,\sigma_c}{\sigma_\tau}\,u_t^\tau,\ (1-\rho^2)\,\sigma_c^2\right).$$

Hence, the joint density function of u^c and u^τ is

$$\begin{aligned} p(u^c, u^\tau \mid \sigma_c^2, \sigma_\tau^2, \rho) \ &\propto\ (\sigma_\tau^2)^{-T/2} \exp\left\{-\frac{1}{2\sigma_\tau^2}\sum_{t=1}^{T}\left(u_t^\tau\right)^2\right\} \\ &\qquad \times\ \left((1-\rho^2)\,\sigma_c^2\right)^{-T/2} \exp\left\{-\frac{1}{2(1-\rho^2)\,\sigma_c^2}\sum_{t=1}^{T}\left(u_t^c - \tfrac{\rho\,\sigma_c}{\sigma_\tau}u_t^\tau\right)^2\right\} \\ &=\ \left((1-\rho^2)\,\sigma_\tau^2\sigma_c^2\right)^{-T/2} \exp\left\{-\frac{1}{2\sigma_\tau^2}k_3 - \frac{1}{2(1-\rho^2)\,\sigma_c^2}\left(k_1 - \tfrac{2\rho\,\sigma_c}{\sigma_\tau}k_2 + \tfrac{\rho^2\sigma_c^2}{\sigma_\tau^2}k_3\right)\right\} \end{aligned}$$

where

$$k_1 = \sum_{t=1}^{T}\left(u_t^c\right)^2, \qquad k_2 = \sum_{t=1}^{T} u_t^c u_t^\tau, \qquad k_3 = \sum_{t=1}^{T}\left(u_t^\tau\right)^2$$

It follows that:

$$p\left(\sigma_c^2 \mid y, \tau, \sigma_\tau^2, \rho, \tau_0, \tau_{-1}\right)\ \propto\ p(\sigma_c^2) \times (\sigma_c^2)^{-T/2}\ \exp\left\{-\frac{1}{2(1-\rho^2)\,\sigma_c^2}\left(k_1 - \tfrac{2\rho\,\sigma_c}{\sigma_\tau}k_2 + \tfrac{\rho^2\sigma_c^2}{\sigma_\tau^2}k_3\right)\right\}$$

where $p(\sigma_c^2)$ is the prior for σ_c^2

Similarly, we can implement step 4 and 5:

$$p\left(\sigma_\tau^2 \mid y, \tau, \sigma_c^2, \rho, \tau_0, \tau_{-1}\right)\ \propto\ p\left(\sigma_\tau^2\right) \times \left(\sigma_\tau^2\right)^{-T/2}\ \exp\left\{-\frac{1}{2\sigma_\tau^2}\,k_3 - \frac{1}{2(1-\rho^2)\,\sigma_c^2}\left(k_1 - \frac{2\rho\sigma_c}{\sigma_\tau}\,k_2 + \frac{\rho^2\sigma_c^2}{\sigma_\tau^2}\,k_3\right)\right\}$$

$$p\left(\rho \mid y, \tau, \sigma_c^2, \sigma_\tau^2, \tau_0, \tau_{-1}\right)\ \propto\ p(\rho) \times (1-\rho^2)^{-T/2}\ \exp\left\{-\frac{1}{2(1-\rho^2)\,\sigma_c^2}\left(k_1 - \frac{2\rho\sigma_c}{\sigma_\tau}\,k_2 + \frac{\rho^2\sigma_c^2}{\sigma_\tau^2}\,k_3\right)\right\}$$

where $p(\sigma_\tau^2)$ and $p(\rho)$ denote the priors for σ_τ^2 and ρ, respectively. The full conditional densities for σ_c^2 and ρ (steps 3 and 5) are nonstandard; to sample from them we use a Griddy–Gibbs step, evaluating each full conditional on a fine grid and drawing via the inverse–transform method (see Kroese, Taimre, and Botev, 2011).

Finally, recall that we can write $\alpha = \mathbf{X}_\delta\,\delta$, where $\delta = (\tau_0, \tau_{-1})'$ and

$$\mathbf{X}_\delta = \begin{pmatrix} 2 & -1 \\ 3 & -2 \\ \vdots & \vdots \\ T+1 & -T \end{pmatrix}.$$

Then

$$\left(\tau \mid u^c, \sigma_c^2, \sigma_\tau^2, \rho, \tau_0, \tau_{-1}\right) \sim \mathcal{N}\left(\mathbf{X}_\delta\,\delta \;+\; \frac{\rho\,\sigma_\tau}{\sigma_c}\,\mathbf{H}_2^{-1}u^c,\; (1-\rho^2)\,\sigma_\tau^2\,(\mathbf{H}_2'\mathbf{H}_2)^{-1}\right),$$

where $u_t^\tau \sim \mathcal{N}(0, \sigma_\tau^2)$.

Given the normal prior for δ,

$$\delta \sim \mathcal{N}(\delta_0,\, \mathbf{V}_\delta), \qquad \mathbf{V}_\delta = \operatorname{diag}(V_\tau, V_\tau), \quad \delta_0 = (\tau_{00}, \tau_{00})',$$

standard regression results yield

$$\left(\tau_0, \tau_{-1} \mid y, \tau, \phi, \sigma_c^2, \sigma_\tau^2, \rho\right) \sim \mathcal{N}\big(\hat{\delta},\; \mathbf{K}_\delta^{-1}\big),$$

with

$$\mathbf{K}_\delta = \mathbf{V}_\delta^{-1} \;+\; \frac{1}{(1-\rho^2)\,\sigma_\tau^2}\,\mathbf{X}_\delta'\,\mathbf{H}_2'\mathbf{H}_2\,\mathbf{X}_\delta,$$

and

$$\hat{\delta} = \mathbf{K}_\delta^{-1}\left(\mathbf{V}_\delta^{-1}\delta_0 + \frac{1}{(1-\rho^2)\,\sigma_\tau^2}\,\mathbf{X}_\delta'\,\mathbf{H}_2'\left[\tau - \frac{\rho\,\sigma_\tau}{\sigma_c}\,\mathbf{H}_2^{-1}u^c\right]\right).$$

Before estimation, we adopt the priors summarized in Table 2.

Table 2: Priors and hyperparameters

Parameters	**Distributions**	**Hyperparameters**
θ	Normal	$\mathcal{N}(\theta_{0,\,2\times1},\, V_{\theta,\,2\times2})\,\mathbf{1}\{\theta \in R\};\ \theta_0 = \begin{bmatrix} 1.3 \\ -0.4 \end{bmatrix};\ V_\theta = \mathbb{I}$
$\tau_0,\ \tau_{-1}$	Normal	$\mathcal{N}(\tau_{00},\, V_\tau);\ \tau_{00} = 390;\ V_\tau = 100$
σ_c^2	*Uniform*	$\mathcal{U}(0, b_c);\ b_c = 4.75$
σ_τ^2	*Uniform*	$\mathcal{U}(0, b_\tau);\ b_\tau = 0.05$
ρ	*Uniform*	Bounded between -1 and 1

The hyperparameters for σ_c^2 and σ_τ^2 were selected using marginal-likelihood (ML) performance as in Chan and Eisenstat (2015). Under Equation (3), σ_τ^2 measures the volatility of innovations to trend growth (i.e., potential–growth shocks). The next figure plots real GDP

alongside its estimated potential level.

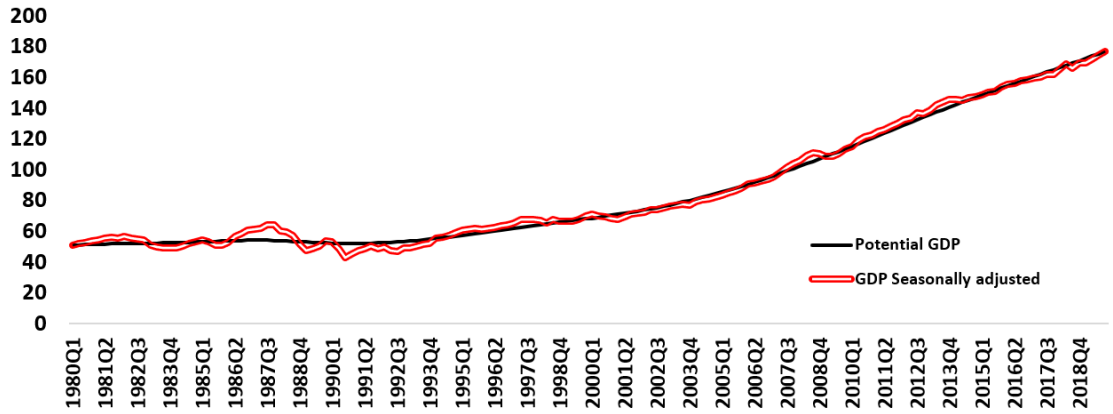

Figure 1: Real GDP: level and estimated potential (UCUR2M–MN)

All results use seasonally adjusted quarterly real GDP for Peru, 1980Q1–2018Q4. Figure 1 plots the GDP level together with its estimated trend. The estimate reveals three distinct phases in trend behavior, consistent with two breaks in trend growth occurring around 1992 and 2003 (see Guillén and Rodríguez (2014) for Peru and Perron and Wada (2009) for the United States). Although the specification does not impose deterministic breakpoints, the methodology is sufficiently flexible to allow trend growth to vary markedly over time . As noted earlier, most alternatives in Table 1 perform less well for Peru, largely because they struggle to accommodate these breaking points.

3. Comparison with alternative UC models

In this subsection, we present results for HP–UC, HP–AR, P-W, UC2M, and UCUR2M. For comparison, we also report an application of Perron's methodology (P–W). Model performance is assessed using statistical criteria and consistency with Peruvian economic history.

3.1. The growth rate of the potential Output:

Before comparing potential–output estimates across methods, we emphasize that validity should be judged against Peru's documented economic history. A trend–cycle decomposition is "well behaved" if it coheres with major historical episodes that plausibly affected potential growth. In Peru, several events are associated with lower GDP growth—and thus lower potential growth—including the 1982–1983 *El Niño* phenomenon[6], during which average *quarterly* real GDP growth was −4.9 percent; the late-1980s/early-1990s hyperinflation,

[6]Similar events occurred in 1997–1998 and 2017, with average annual growth of 3.0 and 2.5 percent, respectively; these appear less detrimental to potential output than the 1982–1983 episode.

with average quarterly growth of −9.6 percent; and the 2000–2001 financial–political crisis, with average quarterly growth of −4.3 percent between 2000Q4 and 2001Q1.

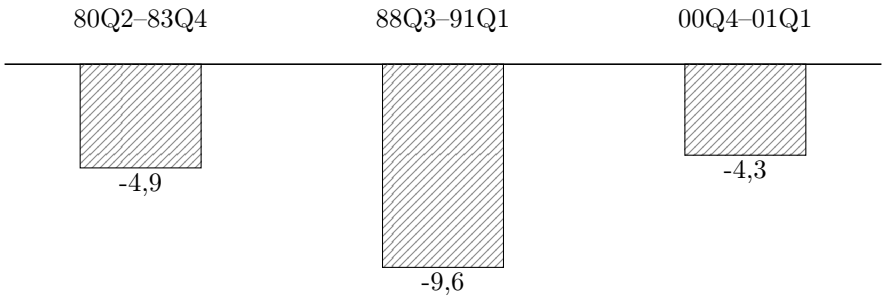

Figure 2: Real GDP Growth – quarterly average

Consistent with the data, Miller (2003) reviews the main trend–cycle decomposition methods and concludes that—regardless of the approach—potential output likely registered negative growth during the late-1980s hyperinflation.

Figure 3 reports potential–growth estimates across the five methodologies considered. The P–W model and HP–AR both show relatively stable growth from 1980 through the early 1990s. By contrast, HP-UC and UC2M indicate negative growth over much of the late 1980s, followed by a recovery in the 1990s. HP–UC delivers a pattern broadly similar to UC2M and UCUR2M, though with greater volatility. From the early 2000s onward, all models display broadly similar dynamics, pointing to a deceleration of potential growth in recent years.

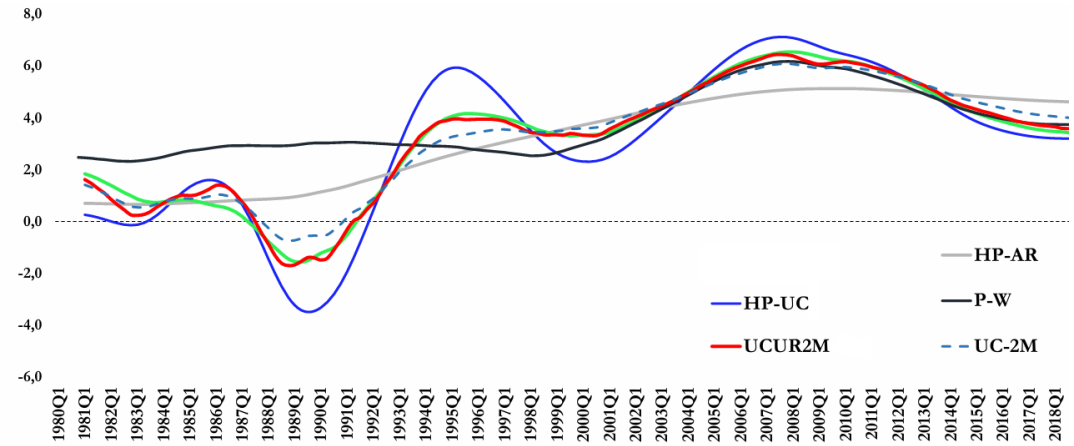

Figure 3: Real GDP Growth - YoY

As noted, the P–W and HP–AR estimates indicate positive, stable potential growth from 1980 through the late 1990s—at odds with Miller (2003) and with the HP–UC, UC2M, and

UCUR2M results, which imply negative potential growth in the late 1980s. This divergence leaves open the question of the qualitative evolution of potential output over that period.

Because potential output is unobservable, its precise evolution cannot be known with certainty. Nonetheless, evidence from GDP growth during these episodes suggests that the deep economic and social crises likely drove potential growth into negative territory, reflecting deterioration of the capital stock, reductions in employment, and adverse effects on total factor productivity.

3.2. Output Gap

Figure 4 compares the estimated output gaps across methods. The P–W model delivers a smaller gap by the late 1980s, consistent with its assumption of positive trend growth in that period. By contrast, the other specifications yield broadly similar gaps of larger magnitude. All approaches indicate a highly volatile and wide gap from the early 1980s through the late 1990s, followed by a marked moderation in both volatility and amplitude over the last two decades of the sample, consistent with a more stable macroeconomic and social environment.

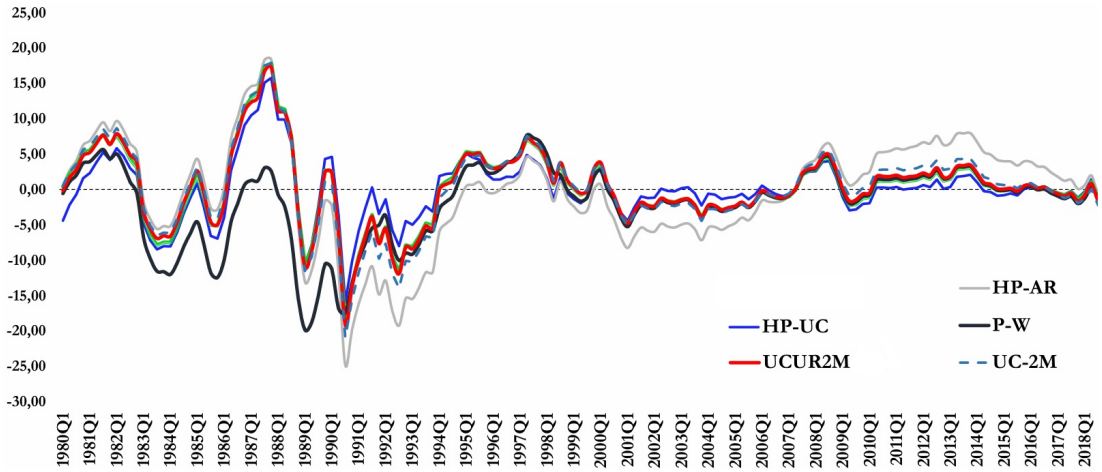

Figure 4: Output gap

Within the framework of Peru's inflation-targeting regime introduced in 2001, monetary policy has helped keep the output gap close to zero. Even so, external conditions have remained a key driver of economic activity, at times amplifying or offsetting domestic stabilization efforts.

Since the onset of the commodity boom (2001–2007), the estimated output gap recovered steadily, peaking in 2008Q4 before turning negative with the global Great Recession. The relatively moderate trough that followed likely reflects Peru's policy buffers—an effective inflation-targeting framework and windfall gains from commodities—which helped cushion the downturn.

Over the period 2000–2018, the output gap has again turned negative—though less so than during the Great Recession. This mild slack is consistent with a less favorable external environment and a moderation of GDP growth driven by structural factors. The level shifts are illustrated in Figure 5.

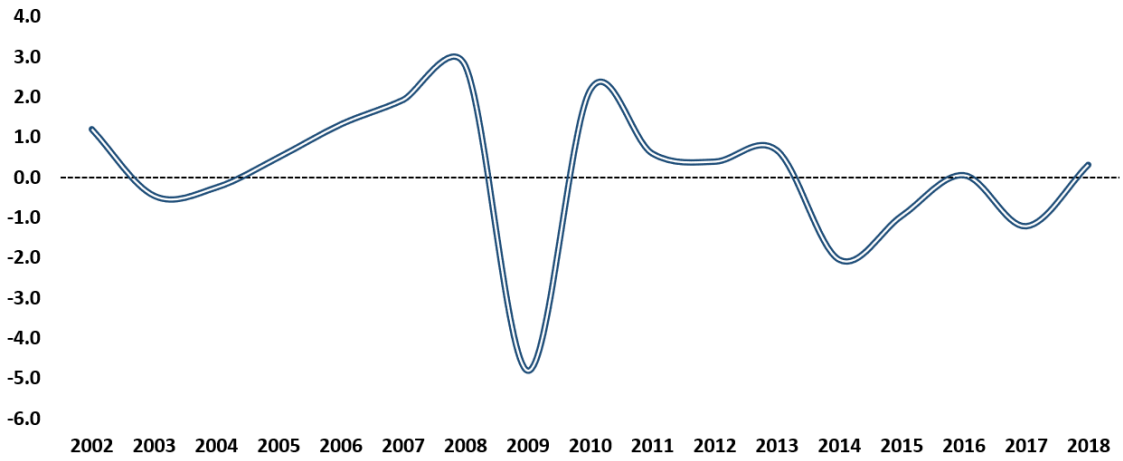

Figure 5: Level change of the output gap

Figures 4 and 5 show that, although the output gap shifted sharply during the Great Recession, its trough was not very deep. In recent years, the gap has moved less, suggesting that its small, persistent negative values are mainly due to weaker external conditions and structural factors.

3.3. Model Comparison:

In Table 3 I report posterior summaries for each methodology, which display broadly similar qualitative behavior of the output gap. Consistent with Chan and Grant (2018a,b) for the United States, when the persistence of the transitory component is estimated, the posteriors are similar regardless of the trend specification.

Table 3: Posterior summaries across models

		HP-UC	HP-AR	UC2M	UCUR2M
ϕ_1	*(mean)*	–	1.33	1.28	1.27
ϕ_1	*(s.d.)*	–	0.07	0.07	0.08
ϕ_2	*(mean)*	–	−0.41	−0.41	−0.41
ϕ_2	*(s.d.)*	–	0.07	0.07	0.07
σ_c^2	*(mean)*	4.73	4.56	4.50	4.49
σ_c^2	*(s.d.)*	0.02	0.16	0.21	0.20
σ_τ^2	*(mean)*	–	–	0.04	0.03
σ_τ^2	*(s.d.)*	–	–	0.02	0.02
ρ	*(mean)*	–	–	–	−0.23
ρ	*(s.d.)*	–	–	–	0.60
τ_0	*(mean)*	397.02	391.93	391.82	392.38
τ_0	*(s.d.)*	0.84	1.99	2.05	2.01
τ_{-1}	*(mean)*	396.95	391.76	391.76	391.98
τ_{-1}	*(s.d.)*	0.94	2.08	0.88	2.35
$\hat{\lambda}$		–	–	129.14	–

The UC2M model is the model that allows the λ estimate as opposed to setting a predetermined value at 1600 as in the HP model. The results show that the estimated λ is very different from the default value for quarterly series.

3.4. Model comparison via integrated likelihood

We compute the integrated likelihood (IL) following Chan and Grant (2018a):

Table 4: Integrated likelihood (log) by model

	HP-UC	HP-AR	UC2M	**UCUR2M**
IL (log)	−709.3	−392.0	−388.8	**−388.0**
s.d.	0.2	0.0	0.1	**0.1**

The UCUR2M model delivers the best statistical performance among the alternatives considered. It also captures key historical features of Peru's economy: (i) negative potential-growth rates in the late 1980s (consistent with the economic and social crisis), (ii) a strong recovery in the early 1990s (following structural reforms), (iii) a moderate slowdown in the late 1990s and early 2000s (amid financial and political turmoil), (iv) an acceleration during the commodity boom (peaking at 6.3 percent in 2007Q4), and (v) a deceleration in potential

growth since the Great Recession (highlighting the need for structural policies to boost growth). Accordingly, We use the UCUR2M output gap to date Peru's business cycle.

4. Identification and dating of business cycles

We define a complete cycle as the interval between consecutive peaks of the cyclical component of GDP. Figure 6 identifies five business cycles—four complete and one ongoing as of 2018Q4 (the end of the sample). Each cycle has two phases: (i) a contraction, from the first peak to the subsequent trough, and (ii) an expansion, from that trough to the next peak (which begins the following cycle). The difference between a cycle's peak and trough is its amplitude, a summary of cyclical volatility.

In terms of volatility, Figure 6 shows a clear shift: business cycles in 1980Q1–1997Q1 exhibit much greater amplitude than those in 1997Q2–2018Q4.

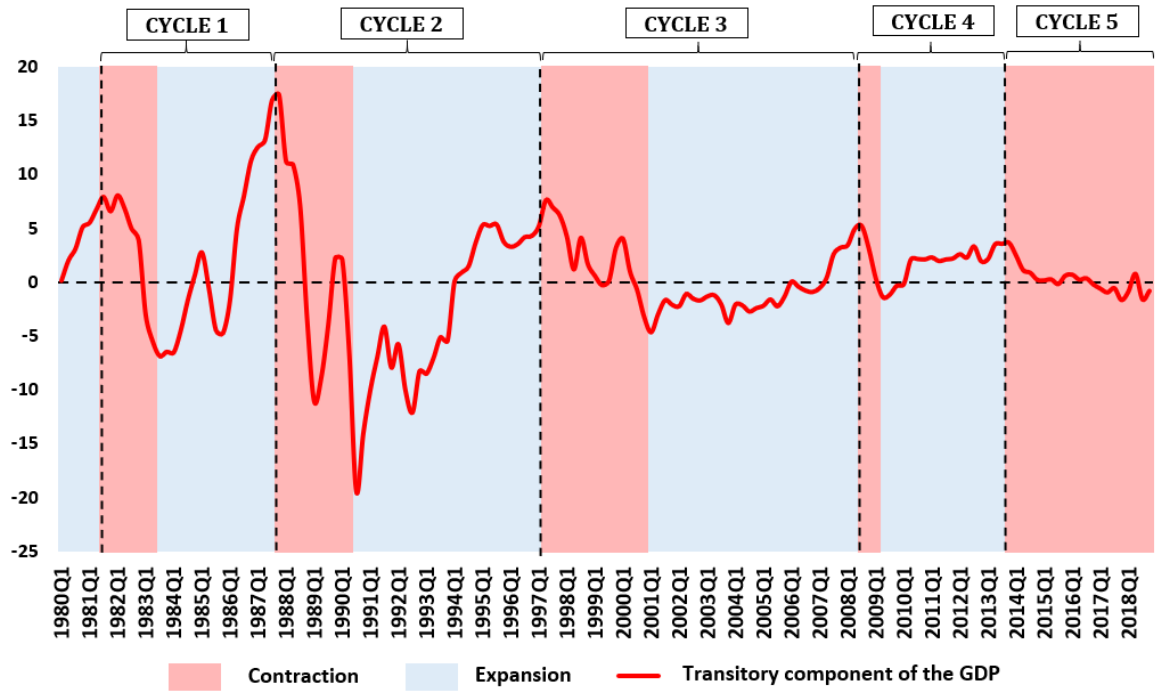

Figure 6: Business cycles and phases

It is also worth noting that the cyclical component declines in every recession since 1980, where a recession is defined as two consecutive quarters of negative growth in seasonally adjusted GDP. Recessions commonly occur during contraction phases, though not every contraction entails a recession. Table 5 quantifies the business cycles depicted in Figure 6. The four complete cycles span 1981Q3–2013Q3, with a maximum duration of 45 quarters for the third cycle (1997Q2–2008Q2) and a minimum of 21 quarters for the fourth (2008Q3–2013Q3).

Table 5: Business cycles: phases, durations, amplitudes, and recessions

Business Cycle					Recessions		
Nº	**Phase**	**Period**	**Duration**	**Max amplitude**	**Nº**	**Period**	**Duration**
Cycle 1		[1981Q3–1987Q3]	25	24.24			
	Contraction	[1981Q3–1983Q2]	8	14.78	Recession 1	[1982Q2–1983Q4]	7
	Expansion	[1983Q3–1987Q3]	17	24.24	Recession 2	[1985Q2–1985Q4]	3
Cycle 2		[1987Q4–1997Q1]	38	36.81			
	Contraction	[1987Q4–1990Q2]	11	36.81	Recession 1	[1987Q4–1989Q1]	6
	Expansion	[1990Q3–1997Q1]	27	27.03	Recession 2	[1990Q2–1990Q3]	2
					Recession 3	[1992Q2–1992Q3]	2
Cycle 3		[1997Q2–2008Q2]	45	12.25			
	Contraction	[1997Q2–2000Q4]	15	12.25	Recession 1	[1998Q1–1999Q1]	5
	Expansion	[2001Q1–2008Q2]	30	9.86	Recession 2	[2000Q2–2001Q1]	4
Cycle 4		[2008Q3–2013Q3]	21	6.60			
	Contraction	[2008Q3–2009Q1]	3	6.60	Recession 1	[2008Q4–2009Q2]	3
	Expansion	[2009Q2–2013Q3]	18	5.03			
Cycle 5		[2013Q4–]	21	5.31			
	Contraction	[2013Q4–]	21	5.31	(optional)	[2014Q1–2014Q2]	2

The standout result is the sharp decline in cyclical volatility beginning in 1997, evident in the smaller peak–to–trough amplitudes. The first two cycles (1981Q3–1997Q1) reach maximum amplitudes above 30 percentage points. Volatility moderates during the contraction of the third cycle (1997Q2–2000Q4) and declines further in its expansion (2001Q1–2008Q2). Notably, the lower-volatility cycles coincide with the post–early-1990s reform period. Beyond the sustained drop in volatility, the frequency of recessions also falls: whereas the first three cycles each contain two to three recessions, the fourth cycle records only one—during the Global Financial Crisis—which is the last observed in the sample.

Table 6 shows that the contraction phases of the first two cycles, periods of high volatility, exhibit negative GDP growth, largely reflecting the economic and social crises of those years. By contrast, subsequent contractions display positive average growth. Across all cycles, expansion phases are characterized by positive average GDP growth.

Table 6: Phase averages by cycle: GDP growth, output gap (average), and potential growth (average)

	Period	GDP growth rates	Output gap (average)	Potential output growth rate (average)
Contraction Periods				
Cycle 1	*[1981Q3 – 1983Q2]*	$-1,6$	$3,7$	$0,7$
Cycle 2	*[1987Q4 – 1990Q2]*	$-5,7$	$1,5$	$-1,2$
Cycle 3	*[1997Q2 – 2000Q4]*	$2,4$	$2,4$	$3,5$
Cycle 4	*[2008Q3 – 2009Q1]*	$4,5$	$2,9$	$6,1$
Cycle 5	*[2013Q4 –]*	$3,4$	$0,2$	$4,1$
Expansion Periods				
Cycle 1	*[1983Q3 – 1987Q3]*	$4,4$	$1,9$	$0,9$
Cycle 2	*[1990Q3 – 1997Q1]*	$3,5$	$-2,9$	$2,3$
Cycle 3	*[2001Q1 – 2008Q2]*	$5,7$	$-1,1$	$5,2$
Cycle 4	*[2009Q2 – 2013Q3]*	$6,0$	$1,7$	$5,8$

A decade-by-decade decomposition of GDP growth into contributions from the output gap and potential output appears in Table 7. Potential growth is weakest in the 1980s, while the gap contributes negatively, reflecting the decade's economic and social crises. In the 1990s, structural reforms support positive contributions from both the trend and the gap. For much of the 2000s, a favorable external environment and the adoption of inflation targeting keep the gap near zero, making potential growth the primary driver of economic activity. In the most recent decade, the contribution of potential growth moderates—consistent with structural headwinds—while short-run stabilization policies have largely kept the gap close to its potential, yielding a small negative contribution from the gap on average.

Table 7: Real GDP growth contributions (% per year)

Years	τ_t	c_t	GDP
1981–1990	0,2	−1,2	−0,7
1991–2000	2,9	1,0	4,0
2001–2010	5,4	0,2	5,6
2011–2018	4,7	−0,4	4,3
1981–2018	3,2	−0,1	3,2

5. Conclusions

This paper estimates GDP's cycle and trend using a purely statistical approach that embeds a simple economic structure: the unit root in GDP arises from its trend, while the cyclical

component is stationary and autoregressive. In particular, the trend's *growth rate* follows a second–order Markov process, in contrast to conventional UC models where the *level* of the trend is a first–order random walk. This specification affords greater flexibility and captures potential breaks in trend growth. The application is implemented within a Bayesian unobserved–components framework, leveraging banded and sparse linear–algebra algorithms for state–space models that are computationally more efficient than Kalman filter–based methods.

Estimates from the UCUR2M model outperform alternative approaches in both statistical fit and alignment with Peru's economic history. The inferred path of potential growth is consistent with the main economic and social episodes over the sample. The output gap exhibits high volatility in the 1980s, moderates during the 1990s, and remains smaller and more stable from the early 2000s onward.

The estimated output gap allows us to date Peru's business cycles. We identify five cycles, four complete and one ongoing as of 2018Q4,with durations ranging from 21 to 45 quarters. Cycles prior to the 1990s are highly volatile, largely reflecting the economic and social crises of that period, whereas more recent cycles exhibit lower volatility consistent with a more stable macroeconomic and social environment.

Regarding GDP growth contributions, the evidence indicates that real growth is driven primarily by potential (trend) growth, with only a small contribution from the output gap. This pattern is consistent with short-term macroeconomic policy keeping the economy close to potential.

References

Baxter, M. and King, R. (1999). Measuring Business Cycles: Approximate Band-Pass Filters For Economic Time Series. *The Review of Economics and Statistics*, 81(4): 575-593.

Beveridge, S. and Nelson, C. (1981). A new approach to decomposition of economic time series into permanent and transitory components with particular attention to measurement of the 'business cycle'. *Journal of Monetary Economics*, 7(2):151–174.

Cabredo, F. and Valdivia, C. (1998). *Estimación del PBI Potencial para el Perú*. Banco Central de Reserva del Perú.

Chan, J. and Eisenstat, E. (2015). Marginal likelihood estimation with the cross-entropy method. *Econometric Reviews*, 34(3):256–285.

Chan, J. and Grant, A. (2018a). A Bayesian model comparison for trend-cycle decompositions of output. *Journal of Money, Credit and Banking*, 50(2–3):525–552.

Chan, J. and Grant, A. (2018b). Reconciling output gaps: Unobserved components model and Hodrick–Prescott filter. *Journal of Economic Dynamics and Control*, 75:114–121.

Chan, J. and Jeliazkov, I. (2009). Efficient simulation and integrated likelihood estimation in state space models. *International Journal of Mathematical Modelling and Numerical Optimisation*, 1:101–120.

Clark, P. K. (1987). The cyclical component of U.S. economic activity. *The Quarterly Journal of Economics*, 102(4):797–814.

Guillén, A. and Rodríguez, G. (2014). Trend–cycle decomposition for Peruvian GDP: application of an alternative method. *Latin American Economic Review*, 23:5.

Hodrick, R. and Prescott, E. (1997). Postwar U.S. business cycles: An empirical investigation. *Journal of Money, Credit and Banking*, 29(1):1–16.

Harvey, A. C. (1985). Trends and cycles in macroeconomic time series. *Journal of Business & Economic Statistics*, 3(3):216–227.

Llosa, L. and Miller, S. (2005). Using additional information in estimating the output gap in Peru: a multivariate unobserved component approach. Working Paper No. 2005-004, Banco Central de Reserva del Perú.

McCausland, W., Miller, S., and Pelletier, D. (2010). Simulation-based likelihood in state space models. *Econometrics Journal*, 13(1):1–23.

Miller, S. (2003). Métodos alternativos para la estimación del PBI potencial: Una aplicación para el caso de Perú. *Revista de Estudios Económicos, BCRP*.

Morley, J., Nelson, C., and Zivot, E. (2003). Why are the Beveridge–Nelson and unobserved-components decompositions of GDP so different? *The Review of Economics and Statistics*, 85(2):235–243.

Perron, P. y Wada, T. (2009). Let's take a break: Trends and cycles in U.S. real GDP. *Journal of Monetary Economics*, 56:749–765.

Rodríguez, G. (2009). Using A Forward-Looking Phillips Curve to Estimate the Output Gap in Peru. Working Paper No. 2009-010, Banco Central de Reserva del Perú.

Chagny, O. y Doepke, J. (2001). Measures of the output gap in the Eurozone: An empirical assessment. *Economic Modelling*, 18(3):555–583.

Watson, M. W. (1986). Univariate detrending methods with stochastic trends. *Journal of Monetary Economics*, 18:49–75.